Europe PMC Funders Group
Author Manuscript
Histochem Cell Biol. Author manuscript; available in PMC 2011 September 29.

Published in final edited form as:
Histochem Cell Biol. 2008 August ; 130(2): 407–419. doi:10.1007/s00418-008-0429-4.

Electron microscopic visualization of fluorescent signals in cellular compartments and organelles by means of DAB-photoconversion

Claudia Meißlitzer-Ruppitsch,
Department of Cell Biology and Ultrastructure Research, Center for Anatomy and Cell Biology, Medical University Vienna, Schwarzspanierstrasse 17, 1090 Vienna, Austria

Monika Vetterlein,
Department of Cell Biology and Ultrastructure Research, Center for Anatomy and Cell Biology, Medical University Vienna, Schwarzspanierstrasse 17, 1090 Vienna, Austria

Herbert Stangl,
Institute of Medical Chemistry, Center for Physiology and Pathophysiology, Medical University of Vienna, Vienna, Austria

Susanne Maier,
Institute of Pharmacology, Center for Biomolecular Medicine and Pharmacology, Medical University of Vienna, Vienna, Austria

Josef Neumüller,
Department of Cell Biology and Ultrastructure Research, Center for Anatomy and Cell Biology, Medical University Vienna, Schwarzspanierstrasse 17, 1090 Vienna, Austria

Michael Freissmuth,
Institute of Pharmacology, Center for Biomolecular Medicine and Pharmacology, Medical University of Vienna, Vienna, Austria

Margit Pavelka, and
Department of Cell Biology and Ultrastructure Research, Center for Anatomy and Cell Biology, Medical University Vienna, Schwarzspanierstrasse 17, 1090 Vienna, Austria

Adolf Ellinger
Department of Cell Biology and Ultrastructure Research, Center for Anatomy and Cell Biology, Medical University Vienna, Schwarzspanierstrasse 17, 1090 Vienna, Austria, adolf.ellinger@meduniwien.ac.at

Abstract

In this work, we show the photoconversion of the fluorochromes enhanced green fluorescent protein (EGFP), yellow fluorescent protein (YFP), and BODIPY into electron dense diaminobenzidine (DAB)-deposits using the examples of five different target proteins, and the lipid ceramide. High spatial resolution and specificity in the localization of the converted protein-fluorochrome complexes and the fluorochrome-labelled lipid were achieved by methodical adaptations around the DAB-photooxidation step, such as fixation, illumination, controlled DAB-precipitation, and osmium postfixation. The DAB-deposits at the plasma membrane and membranous compartments, such as endoplasmic reticulum and Golgi apparatus in combination with the fine structural preservation and high membrane contrast enabled differential

© Springer-Verlag 2008
Correspondence to: Adolf Ellinger.

Europe PMC Funders Author Manuscripts
Europe PMC Funders Author Manuscripts

Europe PMC Funders Author Manuscripts

topographical analyses, and allowed three-dimensional reconstructions of complex cellular architectures, such as *trans*-Golgi–ER junctions. On semithin sections the quality, distribution and patterns of the signals were evaluated; defined areas of interest were used for electron microscopic analyses and correlative microscopy of consecutive ultrathin sections. The results obtained with the proteins golgin 84 (G-84), protein disulfide isomerase (PDI), scavenger receptor classB type1 (SR-BI), and γ-aminobutyric acid (GABA) transporter 1 (GAT1), on one hand closely matched with earlier immunocytochemical data and, on the other hand, led to new information about their subcellular localizations as exemplified by a completely novel sight on the subcellular distribution and kinetics of the SR-BI, and provided a major base for the forthcoming research.

Keywords

DAB-photoconversion; Green fluorescent protein; Yellow fluorescent protein; BODIPY; Golgi apparatus

Introduction

Fluorescent markers, including the classical fluorochromes, green and yellow fluorescent proteins, as well as quantum dots, are indispensable in wide fields of cell biological research, such as immunolocalization of molecules, investigation of transport pathways, and visualization of cell dynamics in living cells (for review Giepmans et al. 2006; Lippincott-Schwartz and Patterson 2003; Yuste 2005; Jyoti et al. 2004). Many questions on subcellular processes addressed in these studies require resolutions beyond the light microscopic level. Such precise localization of molecules within organelles and subcellular structures can only be achieved in the electron microscope, in which on the other hand fluorescent signals cannot be recognized. Hence there is a strong need of methods, which translate the fluorescence signals into signals visible in the electron microscope, and which allow to correlate the light microscopical signals with the respective subcellular structures, where the fluorescent markers are localized. One promising approach to the investigation of subcellular compartmentation during transport and cellular dynamics is the conversion of fluorescent signals into electron dense diaminobenzidine (DAB) precipitates. The underlying photooxidation reaction takes advantage of free oxygen radicals that form upon illumination of fluorochromes, and lead to oxidation of DAB in situ. The oxidized DAB in turn forms networks, which osmium-stained appear as fine granular, dense precipitates at the sites of the former fluorescent signals, well visible in the electron microscope.

The idea to convert non-stable fluorescent marker molecules into insoluble, stable products, which can be processed for electron microscopy, was first realized with lucifer yellow-injected cells in 1982 (Maranto 1982). Originally used for neuronal mapping, the method has been extended to a broader spectrum of fluorescent probes (Sandell and Masland 1988; Von Bartheld et al. 1990; Lübke 1993). In these studies, the reactions have been shown to be successful with all markers tested, thus providing evidence that DAB-photoconversion can be considered a general phenomenon. Using fluorescent lipid derivatives, the method has been further elaborated to fine structural resolution (Pagano et al. 1989). Since then, photoconversion increasingly has become a powerful tool, at first prevalently used in neurosciences (Singleton and Casagrande 1996; De-Miguel et al. 2002; Harata et al. 2001), for tracing lipid molecules in distinct organelles, and for the analysis of membrane traffic and subcellular compartmentation (Pagano et al. 1991; Ladinsky et al. 1994; Martin and Pagano 1994; Dantuma et al. 1998; Fomina et al. 2003).

Different strategies for the further advancement of photoconversion led to the development of refined methods using the membrane probe FM 1–43 (Harata et al. 2001), the green

Europe PMC Funders Author Manuscripts

Europe PMC Funders Author Manuscripts

fluorescent protein (GFP, Grabenbauer et al. 2005), or GFP complexed with tetracysteine tags and labelled with the biarsenical reagent ReAsH (Gaietta et al. 2006). Although GFP is one of the most frequently used fluorochromes and has become a major tool in multiple cell biological studies (for review Lippincott-Schwartz and Patterson 2003; Tsien 1998; Chalfie et al. 1994), there are only two reports using the potency of GFP-photoconversion. One, to study peroxisomal protein import by conversion of GFP fused to a peroxisomal targeting sequence (Monosov et al. 1996), the other, to localize the Golgi enzyme *N*-acetylgalactosaminyl-transferase-2 fused with enhanced GFP (EGFP, Grabenbauer et al. 2005).

In the course of our projects, in which complex subcompartments of the biosynthetic and endocytic cellular pathways are in the center of interest (Pavelka et al. 1998, 2008; Vetterlein et al. 2002, 2003) we were confronted with the need to exactly define the ultrastructural basis of the various light microscopical signals, and to achieve precise subcellular localizations. We report here on our results obtained with photoconversion of fluorescent signals, which enabled to identify the ultrastructural localizations of different kinds of molecules, the proteins golgin 84 (G-84, Bascom et al. 1999), protein disulfide isomerase (PDI, Noiva and Lennarz 1992), scavenger receptor classB type1 (SR-BI, Acton et al. 1994), and γ-aminobutyric acid (GABA) transporter 1 (GAT1, Guastella et al. 1990), tagged either with the fluorochromes EGFP or YFP, and the lipid ceramide (Pagano et al. 1989) labelled with BODIPY. We aimed to gain excellent fine structural preservation combined with clear-cut reaction products as basis for high-resolution electron microscopy, electron tomography, and 3D-analysis of the stained cell compartments. Evaluation and quality control were done at several steps of the preparations, and included the analysis of semithin sections, which allowed correlative microscopy of consecutive sections.

Materials and methods

Cell culture

Human foreskin fibroblasts (FSF), Hela cells and hepato-carcinoma (HepG2) cells (American Type Culture Collection, Rockville, MD, USA), were cultured in minimum essential medium (MEM Eagle, Sigma-Aldrich, St Louis, MI, USA) or in Dulbeccos modified Eagle's medium, respectively (DMEM, Sigma), supplemented with 10% foetal bovine serum (FBS) gold (PAA Laboratories, Linz, Austria), 2 mM L-glutamine (Sigma; PAA Laboratories) and non essential amino acid solution (1:100, Sigma), at 37° in a 95% humidified atmosphere with 5% CO_2.

Stably transfected Chinese Hamster Ovarian cells (CHO) lacking LDL receptor (ldlA7, Kingsley and Krieger 1984*),* expressing high levels of SR-BI fused to EGFP (ldlA7-SR-BI-EGFP, Eckhardt et al. 2004; kindly provided by Deneys R. van der Westhuyzen), were cultured in a 1:1 mixture of DMEM and Ham's F-12 medium (Gibco-BRL, Uxbridge, UK) with 100 units/ml penicillin, 100 mg/ml streptomycin sulphate (PAA Laboratories), 1% geneticin (G-418, MedPro, Vienna, Austria) and supplemented with 5% FBS. 5×10^5 cells were seeded on coverslips and cultured for 48 h before use for experiments.

Human embryonic kidney cells (Hek293), stably transfected with YFP-tagged GABA transporter 1 (YFP-GAT1), were cultured in DMEM supplemented with 10% FBS, 50 μg/ml gentamycin (PAA Laboratories) and 250 μg/ml geneticin. All cells were grown as monolayers and seeded on 13 mm round coverslips 24–48 h before used for further experiments.

Europe PMC Funders Author Manuscripts

Europe PMC Funders Author Manuscripts

Cloning and transfection of cell lines

cDNA sequences of human golgin 84 (G-84) and protein disulfide isomerase (PDI) obtained by PCR, were introduced into pCR 2.1-Topo vector (Invitrogen, Lofer, Austria) and subcloned via *Eco*RI restriction into Mammalian Expression Vector pCI (Promega, Mannheim, Germany), fused to EGFP (EGFP-G-84, EGFP-PDI). Transient transfections were performed with the polycationic lipid Roti-Fect (Roth, Lactan, Graz, Austria) or Lipofectamine 2000 (Invitrogen), when cells were in a subconfluent state, according to the manufacturer's protocol. Twenty-four hours after transfection, cells were used for further experiments. Fibroblasts, HepG2 and Hela cells were transiently transfected with PDI and G-84, CHO cells were stably transfected with SR-BI, and Hek293 cells with GAT1.

BODIPY-C5-ceramide-BSA labelling

BODIPY-cer (Bodipy-FL-C5-ceramide complexed to BSA, Molecular Probes, Invitrogen) was prepared as a 2.5 μM solution by diluting a 0.5 mM stock solution in 1× Hanks buffered salt solution (HBBS, Sigma)/10 mM 4-(2-hydroxyethyl)-1-piperazinethansulfonic acid (HEPES, Gibco). HepG2 and Hela cells were washed twice with phosphate-buffered saline (PBS) and incubated up to 30 min with the BODIPY-cer solution at 4°C, rinsed several times with ice-cold medium and further incubated for indicated periods at 37°. After washing cells with fresh culture medium, they were either prepared for fluorescence microscopy or fixed for photoconversion experiments.

Fluorescence microscopy: live cell imaging

Cells, either expressing EGFP- or YFP-tagged proteins, or labelled with BODIPY-cer, were washed and incubated with pre-warmed PBS. Live cell images and photoconversion were done on a Nikon eclipse TE300 microscope equipped with the appropriate excitation filters.

Diaminobenzidine-photoconversion

EGFP and YFP expressing cells, and cells labelled with BODIPY were fixed with 4% formaldehyde and 0.5% glutaraldehyde in PBS at 4°C for 45 min. Thereafter, DAB-photoconversion was performed as follows: cells were washed with 0.05 M Tris/HCl buffer pH 7.4, and pre-incubated with 1 mg/ml DAB (Sigma) in 0.05 M Tris/HCl buffer, pH 7.4 at room temperature for 30 min. Diaminobenzidine solutions were freshly prepared, filtered through folded filters (Machery-Nagel, Germany) and stored at 4°C. Illumination started in fresh DAB-solutions with a HBO 100-W high-pressure mercury vapour lamp. The following objectives and bleaching times were used: for EGFP and YFP 20× (0.45 NA) or 40× (0.60 NA), 20–50 min; BODIPY was first illuminated with 4× (0.13 NA) for 30 min, followed by 10× (0.25 NA) up to 30 min.

For each target/fluorochrome combination, the fading times, until complete bleaching of the majority of cells, were evaluated. For photoconversion these periods were reduced by 20%. Generally, these steps were done on ice and the DAB-solutions renewed after 15 min each. When the illumination was stopped, the fluorescence almost had faded and in turn, the DAB precipitate had become visible in the LM. After rinsing cells in 0.05 M Tris/HCl pH 7.4, they were stored until further preparation.

Transmission electron microscopy (TEM)

Fixed, DAB-photoconverted cells were washed with distilled water and postfixed in 1% osmium-ferrocyanide (1:1 mixture of 2% osmium tetroxide and 3% potassium ferrocyanide; Merck, Darmstadt, Germany) at room temperature for 15 min followed by 1% veronalacetate buffered osmium tetroxide at 4°C for 30 min. Cells were further processed for routine electron microscopy; after dehydration in a graded series of ethanol (50, 70, 90,

Europe PMC Funders Author Manuscripts

Europe PMC Funders Author Manuscripts

96, 100%), they were embedded in Epon (Serva, Heidelberg, Germany). Sections (80–100 nm) of Epon-embedded cells were cut with an UltraCut-UCT ultramicrotome (Leica Inc., Vienna, Austria), transferred to copper grids, and viewed either unstained or stained with uranyl acetate and lead citrate with a Tecnai-20 transmission electron microscope at 80 kV (Tecnai-20 LaB6, FEI Company, Eindhoven, The Netherlands). Digital images were recorded using a slow-scan CCD camera (MSC 794, 1 k × 1 k pixel, Gatan Inc., Pleasanton, CA, USA).

Electron tomography (ET)

Two-hundred-nanometers thick sections of the Epon-embedded probes were cut in parallel to the plane of the cell monolayer and transferred to copper grids. Tomography was performed at 200 kV (Tecnai-20) using a tilting stage, with a high tilt rotation tomography holder (Gatan) to orientate Golgi stacks parallel to the tilting axis. Series with an angular range of typically −65° to +65° were recorded with a tilt increment of 1° using the Gatan slow-scan camera. Individual series were recorded automatically with the Xplore3D software (FEI Company). Before acquisition of tilt series, the software requires a holder calibration procedure, where the dislocation and the defocus of single tilt images are recorded. In addition, an automatic adjustment of the eucentric height and an autofocus procedure is performed. During acquisition of tilted images, dislocations caused by the mechanical imprecision of the stage are corrected. Furthermore, a fine tuning is performed by tracking any individual image by correction using cross-correlation. The images were aligned by using several itinerative cycles of cross correlation and the volume of the sections was reconstructed into serial slices using the software package Inspect 3D (FEI Company). Reconstruction was performed by the weighted projection method. The 3D-model was constructed by tracing the structures of interest on all slices with coloured membrane contours that are merged in the Z axis by Amira 4.1 software (Mercury Computer Systems, Merignac, Cedex, France). Virtual slices were approximately 2-nm thick.

Results

By means of photoconversion, light microscopical fluorescent signals were converted into electron dense DAB-deposits for detailed analyses in the electron microscope. To define appropriate conditions of illumination and conversion, fading of the fluorochromes and growing of the DAB-depositions were controlled under the microscope. During illumination, concomitantly with the decrease of fluorescence, a brown spot arose at the exposed regions pointing to DAB-depositions (Fig. 1). All three fluorochromes, EGFP, YFP and BODIPY, could be successfully converted into distinct DAB-precipitates visible in the electron microscope.

Establishment of the protocol

To achieve distinct reaction products of high-electron density together with high membrane contrast, the influence of parameters, like DAB-concentration and duration of DAB-preincubation, conditions of illumination and post-illumination treatments were tested. Variations in the DAB-preincubation step (0.5–2.0 mg/ml DAB; duration of DAB-preincubation 5–60 min) pointed to a practicable combination of 1 mg/ml and 30 min preincubation, concurrent with the literature. Enhancement of both parameters did not significantly improve the results, but led to an increase of diffuse DAB-depositions. The duration of the illumination was adapted to the respective fluorochrome, and generally was stopped before complete fading. At first, radiation times and end points were determined; in the actual experiments, the times were reduced, cutting off the last 10–20%. In our systems, individual lengths were 20 min for YFP, 45 min for BODIPY, and 20–50 min for EGFP, depending on the primary fluorescence of the cultured cells. The consecutive use of

Europe PMC Funders Author Manuscripts

Europe PMC Funders Author Manuscripts

osmium-ferrocyanide and veronalacetate-buffered osmium tetroxide for postfixation produced optimal contrast of membranes and DAB-deposits (e.g. Fig. 4).

Semithin sections informed about the overall distribution of the precipitate and the quality of the signal conversion. On light microscopical overviews, the reaction patterns within the samples were listed, differences evaluated, and areas of interest for further electron microscopic analyses defined (Fig. 2). These analyses also indicated an increasing amount of DAB-deposits with the duration of the illumination. In addition, the percentage of cells with extremely intense reactions increased (Fig. 2b, c); in the electron microscope, these cells proved to be damaged. Defined regions were correlatively followed on consecutive sections in the electron microscope (Fig. 3). Light microscopically, the stained organelles could not be clearly identified (Fig. 3a, b), and cells with similar light microscopic staining patterns proved to contain differently labelled compartments (Fig. 3c, d), thus underlining the necessity of electron microscopic approaches. The specificity of the conversion step was verified by several controls: EGFP- and YFP, expressing cells and BODIPY-cer labelled cells were incubated with DAB without bleaching and vice versa; in addition, native control cultures devoid of fluorochromes were analyzed. In none of these controls, reactions were observed.

Localization of converted fluorescent signals in cellular compartments

EGFP-tagged scavenger receptor BI—EGFP-SR-BI expressing ldlA7cells showed fluorescence at the plasma membrane (PM) and in distinct cellular areas. The light microscopical image alone did not allow to identify the stained organelles (Fig. 4a; Eckhardt et al. 2004). In the electron microscope, distinct DAB-deposits marked the PM, endosomes, the ER and the Golgi apparatus (Fig. 4b–e). Remarkably, in the Golgi apparatus, clear cut deposits were apparent only in 1–2 cisternae either at the *cis*, medial, or *trans* parts of the stacks, or in the TGN (Fig. 4b, c). Within the ER, two staining patterns prevailed: reaction products either marked limited regions of ER cisternae in a “mosaic-like pattern” (Fig. 4d), or homogeneously filled the entire ER (Fig. 4e). Strikingly, reaction products were never found within the nuclear envelope, which always remained negative (Fig. 4b, c, e). Control samples showed no reaction products (Fig. 4f).

EGFP-tagged G-84 and PDI in fibroblasts and hepatoma cells—The fluorescent signals of G-84 were concentrated in a perinuclear tubulo-reticular network, corresponding to the localization of the Golgi apparatus (Fig. 5a). On the contrary, the PDI-signals were homogeneously distributed in the cytoplasm (Fig. 5b); co-expression of EGFP-G-84 and EGFP-PDI showed both, the perinuclear and the cytoplasmic staining (Fig. 5c). After photoconversion, the DAB-reaction products of G-84 were found exclusively in the Golgi apparatus, thus defining the light microscopical image. The reaction products were not uniformly distributed, but found in a polar position, labelling the utmost cisterna at one side of the stacks, and here being concentrated within distinct segments (Fig. 5d). After co-expression of EGFP-PDI and EGFP-G-84, the deposits on the one hand labelled the nuclear envelope and the ER, and on the other hand Golgi membranes (Fig. 5e).

YFP-tagged γ-aminobutyric acid transporter 1 in Hek293 cells—GAT1 showed strong fluorescence at the PM of the HEK293 cells; the labelling was especially pronounced at the microvilli (Fig. 6a). The corresponding ultrastructural image confirmed the reaction products at the plasma membranes (Fig. 6b). Controls exhibited no staining (insert).

BODIPY-cer in human fibroblasts

Time-dependent uptake—To follow the time-dependent uptake and intracellular fate of BODIPY-cer, FSF and Hela cells were incubated with BODIPY-cer at 4°C for 30 min, and

Europe PMC Funders Author Manuscripts

Europe PMC Funders Author Manuscripts

post-incubated for different periods at 37°C. The live cell images showed a rapid uptake and accumulation in the Golgi area within minutes (Fig. 7): after rewarming, a slight diffuse fluorescence over the PM and the cytoplasm pre-dominated at 1 min, with a faint perinuclear staining at this early stage (Fig. 7a). With time, increasing fluorescence marked the perinuclear region, then displaying a typical Golgi staining pattern (Fig. 7b–f). This further expressed at 30 min postincubation in a constant perinuclear tubulo-reticular Golgi staining (Fig. 8d). The increasingly intense Golgi reactions were paralleled by a decrease of the diffuse fluorescence.

Ultrastructural analysis of BODIPY-cer labelled Golgi membranes—

Photoconversion of the BODIPY-signals obtained after binding and short-time uptake showed weak staining at the PM, whilst intracellular membranes remained unstained (not shown). Within 10 min, ceramide accumulated at the *trans*-Golgi side. Distinct reaction products were found at the *trans*-Golgi network and in *trans*-Golgi cisternae (Fig. 8a, b), while the *trans*-Golgi ER was devoid of staining (Fig. 8b). Similar to the images after 10-min post-incubation at 37°C, the reactions were concentrated at the *trans*-Golgi side after 30 min. *Trans*-Golgi cisternae and the TGN including vesicle-like structures showed a specific and intense staining (Fig. 8c). Controls were free of reactions.

3D-reconstruction of a trans-Golgi–ER junction after BODIPY-cer labelling—

The clear-cut reaction products in subcellular compartments obtained after photoconversion proved to be particularly valuable for electron tomographic studies. Two-hundred-nanometer thick sections of Epon-embedded photoconverted HeLa cells after uptake of BODIPY-cer for 10 min (see Fig. 8a, b) were used for tomographic analyses of the *trans*-Golgi-ER junctional region. Thanks to the intense photoconversion reactions, the BODIPY-cer-positive *trans*-Golgi/TGN cisternae were clearly discernible from the negative ER membranes localized closely apposed. Figure 9 shows a virtual slice with and without coloured contours (Fig. 9a, b), and 2 different aspects of the 3D-model (Fig. 9c, d). One positive Golgi cisterna has been coloured in green, the unstained ER cisterna in pink. The 3D-reconstructions allowed much more precise analyses as were possible with the conventional two-dimensional view, and provided insight into details of the complex helical organization of the *trans*-Golgi–ER junction.

Discussion

By means of fluorochrome-based precipitation of DAB, we have shown precise subcellular localizations of target proteins and lipids. Using the fluorochromes EGFP, YFP and BODIPY as source for the photoconversion step, clear-cut DAB-reaction products within organelles and membranous compartments, such as endoplasmic reticulum and Golgi apparatus, in combination with high-quality fine structural preservation enabled topographical analyses of molecules far above the resolution of the primary fluorescence signal. Since fluorochromes themselves are not directly visible in the electron microscope, dyes, compatible with both forms of microscopy, and methods for translation of fluorescent signals into electron dense markers were looked for. In 1982, Maranto was the first, by using the classical cytochemical approach of DAB-precipitation (Graham and Karnovsky 1966; for review Fahimi and Baumgart 1999), to show the fluorochrome-based photooxidation of DAB. In the sequel, this principle was refined in diversified methods, like the adaptation for the intrinsically fluorescent protein GFP. The usability of GFP for photoconversion has been discussed controversially. In this respect, the protein shell around the chromophore was thought to prevent oxygen passage and thus, to prevent reactive oxygen species (ROS) generation (Adams et al. 2002; Gaietta et al. 2002). On the other hand, illuminated GFP has been shown to produce singlet oxygen (Greenbaum et al. 2000), as has the photooxidation capacity been used for DAB-precipitation (Monosov et al. 1996), and been further

Europe PMC Funders Author Manuscripts

Europe PMC Funders Author Manuscripts

developed for correlative microscopy and electron tomography (Grabenbauer et al. 2005). This controversy also involves GFP-based chromophore-assisted light inactivation (CALI): GFP has been found to be effective (Rajfur et al. 2002), exhibiting relatively poor efficiency (Surrey et al. 1998) or being ineffective (Tour et al. 2003). Our objective was the localization of different fluorochrome-tagged proteins and fluorochrome-labelled lipids following photooxidation with high-spatial resolution and sensitivity. To achieve these goals, several steps, the photoconversion itself, as well as pre- and postconversion treatments were adapted, essentially setting up on the work by Grabenbauer et al. 2005. In the center stage was the control of the DAB-depositions, which we handled based on our experiences with HRP-DAB-labelling techniques (for review Pavelka and Ellinger 1989; Pavelka et al. 2008). The single steps were developed and checked in the course of projects, in which questions as to the subcellular locations and pathways of molecules suffered from the insufficient resolutions of the fluorescent signals, which by photoconversion could be raised to electron microscopic levels.

Fixation conditions, illumination, and photoconversion

Looking for parameters to improve the DAB-depositions, we correlated published data with own protocols and experiences. In general, variables such as intensity of the primary fluorescence signal, illumination and speed of the optical system, and transmittance of supports (coverslips, Petri dishes, etc.), complicated a comparison of the protocols. For fixation, a modified Karnovsky's-fixative provided enough stability and fine structural details without the necessity of quenching background fluorescence when using higher glutaraldehyde concentrations. Photoconversion has been shown to be oxygen dependent. Additional oxygen supply mainly resulted in accelerated oxidation and reduced irradiation times, such, that the conversion process usually was reduced to about half of the time (Kacza et al. 1997). Equilibration of DAB-solutions with pure N_2 during irradiation has been shown to block completely the DAB-photoconversion, thus pointing to the importance of oxygen (Sandell and Masland 1988). In our systems, oxygen influx only slightly influenced the results, most likely due to sufficient O_2 exchange at the large surface and small volume ratio of the medium covering the cell monolayers (Deerinck et al. 1994). The conversion step itself usually was efficient after 20–30 min. However, since we tried to use the maximum yield of the fluorescence, our illumination times were correlated with the fading of the fluorochrome, shortened by that last segment of minor fluorescence. For amplification of the DAB-signals and simultaneous staining of membranes, the two-step osmification (osmium-ferrocyanide and osmium-veronalacetate) proved most suitable. Thus, for instance, local differences in the SR-BI-labelling of the ER, mosaic patterns on one hand and homogeneous distribution on the other hand, became evident.

Cell biological applications

The survey of the recorded cell biological data obtained with the different systems shows on the one hand the close match with earlier data, mostly achieved with other methods like immunocytochemistry, and on the other hand, provides completely new information about the subcellular localization of the target molecules.

Protein disulfide isomerase, as a molecular chaperon, plays a major role in ER quality control (Noiva and Lennarz 1992; Ni and Lee 2007). Characterized by its KDEL sequence, PDI is a resident ER protein (Munro and Pelham 1987) that was shown highly concentrated in the ER cisternae (Hillson et al. 1984; Morris and Varandani 1988). Since PDI has been well characterized, the subcellular localization defined, and the molecule generally expressed at high levels, we have chosen it to establish the method in our initial experiments together with the Golgi marker G-84. Golgin 84, a member of the golgin family of coiled-coil proteins, is a rab1 binding partner and implicated in tethering vesicles to the Golgi

Europe PMC Funders Author Manuscripts

Europe PMC Funders Author Manuscripts

membranes, as well as Golgi membranes to each other (Bascom et al. 1999; Diao et al. 2003; Satoh et al. 2003). Although rab1 binds to the *cis*-Golgi, the exact localization of G-84 within the Golgi apparatus, *cis*-or-*trans* oriented, has been interpreted diverging (Diao et al. 2003; Satoh et al. 2003). Our G-84 staining concurred with these immunocytochemical data insofar, as the converted signal also was found limited to one side of the stack. Both, G-84 and PDI are good candidates helping to further characterize the membrane systems at the *trans*-Golgi side, above all to delineate between Golgi and ER-membranes. During establishing of the method, co-expression of the two proteins was induced in order to achieve more pronounced fluorescence signals at the low transient transfection rates. Hence, the discrete Golgi staining was used as key indicator for successful photoconversion. Though the co-expressed, converted PDI and G-84 signals were not distinguishable from each other in the Golgi areas, both could be converted and confirmed the success of the method.

The neurotransmitter transporter GAT1, a member of the SLC6 gene family, is known to be located in the plasma membrane (Schmid et al. 2001; Farhan et al. 2007). The SLC6 family of proteins acts as speciWc transporters for neurotransmitters, amino acids, betaine, taurine, and creatine (Höglund et al. 2005). GAT1 was tagged to YFP, and expressed in Hek 293 cells for studies on details of the secretory pathway (Schmid et al. 2001; Farhan et al. 2007). The converted signals apparent at the PM confirmed the light microscopical data, and proved the usefulness of YFP for photoconversion.

Fluorochrome-conjugated sphingolipids have been shown to be suitable dyes for tracing endocytic and nonendocytic transport mechanisms in living cells (Martin and Pagano 1994), and have been used as structural markers of the Golgi apparatus (Pagano et al. 1991). The accumulation of ceramide-bound BODIPY at the *trans*-Golgi side allowed the further definition of this compartment at the ultrastructural level (Pagano et al. 1989,1991; Ladinsky et al. 1994,1999). Based on these studies, we adapted the method to investigate the time-dependent uptake of cer-BODIPY in the live cell microscope, and after photoconversion, the corresponding ultrastructural distribution in the Golgi apparatus and, at the *trans*-Golgi-ER junction. The accumulation in the *trans*-Golgi membranes within 1–30 min after onset of incubation results from metabolizing the insertion of ceramide into sphingomyelin via the activity of the sphingomyelin synthase (Voelker and Kennedy 1982; Merrill and Jones 1990; Huitema et al. 2004), and as a consequence of diffusion and permanent membrane transport processes. In the present work, the clear-cut delineation of the cer-BODIPY-positive *trans*-Golgi cisternae from the negative ER-membranes considerably facilitated electron tomography analyses of the *trans*-Golgi areas. The 3D-reconstructions revealed detailed novel insights into the complex helical organization of the *trans*-Golgi–ER junctions.

The high density lipoprotein (HDL)-receptor SR-BI mediates selective cholesterol uptake (Acton et al. 1994,1996; Krieger 2001), and recycles back to the PM (Pagler et al. 2006). In CHO cells expressing EGFP-SR-BI at high levels and lacking LDL-receptor activity, the receptor is mainly localized on the cell surface, and preferentially associated with caveolae-rich membrane regions, as determined by immunofluorescence and cell fractionation (Babitt et al. 1997; Eckhardt et al. 2004). The intracellular distribution of SR-BI, however, remained completely unclear, and could not be differentiated at the LM level (Eckhardt et al. 2004). Our ultrastructural photoconversion data obtained with these cells not only confirmed the surface localization of the SR-BI but, for the first time, allowed to define its intracellular distribution. It became evident that intracellularly, the receptor is localized in different compartments of both the endosomal and secretory systems, including endosomes, the ER and the Golgi apparatus. These unexpected results, which even could be further refined by characterization of SR-BI-positive ER-subcompartments contrasting to the negative nuclear

Europe PMC Funders Author Manuscripts

Europe PMC Funders Author Manuscripts

envelope, led to a novel sight on the SR-BI-localizations and dynamics with consequences on the design of our further projects.

In this work, we show our experiences with the DAB-photoconversion technique. We report on critical technical steps, pitfalls, methodical developments, and the wide practicability of the method in cell biological projects. Combining the benefits of fluorescence techniques, live cell, and electron microscopy, the usage of the DAB-photoconversion approach led to new insights into organization and architectures of cell compartments, to a completely novel sight on the kinetics of one of the molecules studied, the SR-BI, and provided a major base for forthcoming research.

Acknowledgments

The authors gratefully acknowledge the valuable technical assistance of Mrs.Elfriede Scherzer, and Mrs.Beatrix Mallinger, and like to thank Mr.Ulrich Kaindl for the excellent work done in connection with the 3D-modelling, and the preparation of the figures. Parts of the work were supported by the Austrian Science Foundation (FWF) grant P20116-B11, and SFB 35.

References

Adams SR, Campbell RE, Gross LA, Martin BR, Walkup GK, Yao Y, Llopis J, Tsien RY. New biarsenical ligands and tetracysteine motifs for protein labelling in vitro and in vivo: synthesis and biological applications. J Am Chem Soc. 2002; 124:6063–6076. [PubMed: 12022841]

Acton S, Scherer PE, Lodish HF, Krieger M. Expression cloning of SR-BI, a CD36-related class B scavenger receptor. J Biol Chem. 1994; 269:21003–21009. [PubMed: 7520436]

Acton S, Rigotti A, Landschulz KT, Xu S, Hobbs HH, Krieger M. Identification of scavenger receptor SR-BI as high density lipoprotein receptor. Science. 1996; 271:518–520. [PubMed: 8560269]

Babitt J, Trigatti B, Rigotti A, Smart EJ, Anderson RG, Xu S, Krieger M. Murine SR-BI, a high density lipoprotein receptor that mediates selective lipid uptake, is N-glycosylated and fatty acylated and colocalizes with plasma membrane caveolae. J Biol Chem. 1997; 272:13242–13249. [PubMed: 9148942]

Bascom RA, Srinivasan S, Nussbaum RL. Identification and characterization of Golgin-84, a novel Golgi integral membrane protein with a cytoplasmic coiled-coil domain. J Biol Chem. 1999; 274:2953–2962. [PubMed: 9915833]

Chalfie M, Tu Y, Euskirchen G, Ward WW, Prasher DC. Green fluorescent protein as a marker for gene expression. Science. 1994; 263:802–805. [PubMed: 8303295]

Dantuma NP, Pijnenburg MA, Diederen JH, Van der Horst DJ. Electron microscopic visualization of receptor-mediated endocytosis of DiI-labeled lipoproteins by diaminobenzidine photoconversion. J Histochem Cytochem. 1998; 46:1085–1090. [PubMed: 9705975]

Deerinck TJ, Martone ME, Lev-Ram V, Green DP, Tsien RY, Spector DL, Huang S, Ellisman MH. Fluorescence photooxidation with Eosin: a method for high resolution immunolocalization and in situ hybridization detection for light and electron microscopy. J Cell Biol. 1994; 126:901–910. [PubMed: 7519623]

De-Miguel FF, Muller KJ, Adams WB, Nicholls JG. Axotomy of single fluorescent nerve fibres in developing mammalian spinal cord by photoconversion of diaminobenzidine. J Neurosci Methods. 2002; 117:73–79. [PubMed: 12084566]

Diao A, Rahman D, Pappin DJ, Lucocq J, Lowe M. The coiled-coil membrane protein golgin-84 is a novel rab effector required for Golgi ribbon formation. J Cell Biol. 2003; 160:201–212. [PubMed: 12538640]

Eckhardt ERM, Cai L, Sun B, Webb NR, Van der Westhuyzen DR. High density lipoprotein uptake by scavenger receptor SR-BII. J Biol Chem. 2004; 279:14372–14381. [PubMed: 14726519]

Fahimi HD, Baumgart E. Current cytochemical techniques for the investigation of peroxisomes: a review. J Histochem Cytochem. 1999; 47:1219–1232. [PubMed: 10490450]

Europe PMC Funders Author Manuscripts

Farhan H, Reiterer V, Korkhov VM, Schmid JA, Freissmuth M, Sitte HH. Concentrative export from the endoplasmic reticulum of the γ-aminobutyric acid transporter 1 requires binding to SEC24D. J Biol Chem. 2007; 282:7679–7689. [PubMed: 17210573]

Fomina AF, Deerinck TJ, Ellisman MH, Cahalan MD. Regulation of membrane trafficking and subcellular organisation of endocytic compartments revealed with FM1–43 in resting and activated human T cells. Exp Cell Res. 2003; 291:150–166. [PubMed: 14597416]

Gaietta GM, Deerinck TJ, Adams SR, Bouwer J, Tour O, Laird DW, Sosinsky GE, Tsien RY, Ellisman MH. Multicolor and electron microscopic imaging of connexin trafficking. Science. 2002; 296:503–507. [PubMed: 11964472]

Gaietta GM, Giepmans BN, Deerinck TJ, Smith WB, Ngan L, Llopis J, Adams SR, Tsien RY, Ellisman MH. Golgi twins in late mitosis revealed by genetically encoded tags for live cell imaging and correlated electron microscopy. Proc Natl Acad Sci USA. 2006; 103:17777–17782. [PubMed: 17101980]

Giepmans BN, Adams SR, Ellisman MH, Tsien RY. The fluorescent toolbox for assessing protein location and function. Science. 2006; 312:217–224. [PubMed: 16614209]

Grabenbauer M, Geerts WJ, Fernadez-Rodriguez J, Hoenger A, Koster AJ, Nilsson T. Correlative microscopy and electron tomography of GFP through photooxidation. Nat Methods. 2005; 2:857–862. [PubMed: 16278657]

Graham RC Jr, Karnovsky MJ. The early stages of absorption of injected horseradish peroxidase in the proximal tubules of mouse kidney: ultrastructural cytochemistry by a new technique. J Histochem Cytochem. 1966; 14:291–302. [PubMed: 5962951]

Greenbaum L, Rothmann C, Lavie R, Malik Z. Green fluorescent protein photobleaching: a model for protein damage by endogenous and exogenous singlet oxygen. J Biol Chem. 2000; 381:1251–1258.

Guastella J, Nelson N, Nelson H, Czyzyk L, Keynan S, Miedel MC, Davidson N, Lester HA, Kanner BI. Cloning and expression of a rat brain GABA transporter. Science. 1990; 249:1303–1306. [PubMed: 1975955]

Harata N, Ryan TA, Smith SJ, Buchanan J, Tsien RW. Visualizing recycling synaptic vesicles in hippocampal neurons by FM 1–43 photoconversion. Proc Natl Acad Sci. 2001; 98:12748–12753. [PubMed: 11675506]

Hillson DA, Lambert N, Freedman RB. Formation and isomerization of disulfide bonds in proteins: protein disulfide-isomerase. Method Enzymol. 1984; 107:281–194.

Höglund P, Adzic D, Scicluna SJ, Lindblom J, Fredriksson R. The repertoire of solute carriers of family 6: identification of new human and rodent genes. Biochem Biophys Res Commun. 2005; 336:175–189. [PubMed: 16125675]

Huitema K, Van den Dikkenberg J, Brouwers JF, Holthuis JC. Identification of a family of animal sphingomyelin synthases. EMBO J. 2004; 23:33–44. [PubMed: 14685263]

Jyoti K, Simon J, Simon SM. Potentials and pitfalls of fluorescent quantum dots for biological imaging. Trends Cell Biol. 2004; 14:497–504. [PubMed: 15350978]

Kacza J, Härtig W, Seeger J. Oxygen-enriched photoconversion of fluorescent dyes by means of a closed conversion chamber. J Neurosci Methods. 1997; 71:225–232. [PubMed: 9128160]

Kingsley DM, Krieger M. Receptor-mediated endocytosis of low density lipoprotein: somatic cell mutants define multiple genes required for expression of surface-receptor activity. Proc Natl Acad Sci USA. 1984; 81:5454–5458. [PubMed: 6089204]

Krieger M. Scavenger receptor class B type I is a multiligand HDL receptor that influences diverse physiologic systems. J Clin Invest. 2001; 108:793–797. [PubMed: 11560945]

Ladinsky MS, Kremer JR, Furcinitti PS, McIntosh JR, Howell KE. HVEM tomography of the *trans*-Golgi network: structural insights and identification of a lace-like vesicle coat. J Cell Biol. 1994; 127:29–38. [PubMed: 7929568]

Ladinsky MS, Mastronarde DN, McIntosh JR, Howell KE, Staehelin LA. Golgi structures in three dimensions: functional insights from the normal rat kidney cell. J Cell Biol. 1999; 144:1135–1149. [PubMed: 10087259]

Lippincott-Schwartz J, Patterson GH. Development and use of fluorescent protein markers in living cells. Science. 2003; 300:87–91. [PubMed: 12677058]

Europe PMC Funders Author Manuscripts

Lübke J. Photoconversion of diaminobenzidine with different fluorescent neuronal markers into a light and electron microscopic dense reaction product. Microsc Res Tech. 1993; 1:2–14.

Maranto AR. Neuronal mapping: a photooxidation reaction makes lucifer yellow useful for electron microscopy. Science. 1982; 217:953–955. [PubMed: 7112109]

Martin OC, Pagano RE. Internalization and sorting of a fluorescent analogue of glucosylceramide to the Golgi apparatus of human skin fibroblasts: utilization of endocytic and nonendocytic transport mechanisms. J Cell Biol. 1994; 125:769–781. [PubMed: 8188745]

Merrill AH, Jones DD. An update of enzymology and regulation of sphingomyelin metabolism. Biochim Biophys Acta. 1990; 1044:1–12. [PubMed: 2187537]

Monosov EZ, Wenzel TJ, Lüers GH, Heyman JA, Subramani S. Labeling of peroxisomes with green fluorescent protein in living *P. pastoris* cells. J Histochem Cytochem. 1996; 44:581–589. [PubMed: 8666743]

Morris JI, Varandani PT. Characterization of a cDNA for human glutathione-insulin transhydrogenase (protein-disulfide isomerase/oxidoreductase). Biochim Biophys Acta. 1988; 949:169–180. [PubMed: 3342239]

Munro S, Pelham HR. A c-terminal signal prevents secretion of luminal ER proteins. Cell. 1987; 48:899–907. [PubMed: 3545499]

Ni M, Lee AS. ER chaperones in mammalian development and human diseases. FEBS Lett. 2007; 581:3641–3651. [PubMed: 17481612]

Noiva R, Lennarz WJ. Protein disulfide isomerase: a multifunctional protein resident in the lumen of the endoplasmic reticulum. J Biol Chem. 1992; 267:3553–3556. [PubMed: 1740407]

Pagano RE, Sepanski MA, Martin OC. Molecular trapping of a fluorescent ceramide analogue at the Golgi apparatus of fixed cells: interaction with endogenous lipids provides a *trans*-Golgi marker for both light and electron microscopy. J Cell Biol. 1989; 109:2067–2079. [PubMed: 2478562]

Pagano RE, Martin OC, Kang HC, Haugland RP. A novel fluorescent ceramide analogue for studying membrane traffic in animal cells: accumulation at the Golgi apparatus results in altered spectral properties of the sphingolipid precursor. J Cell Biol. 1991; 113:1267–1279. [PubMed: 2045412]

Pagler TA, Rhode S, Neuhofer A, Laggner H, Strobl W, Hinterndorfer C, Volf I, Pavelka M, Eckhardt ER, Van der Westhuyzen DR, Schütz GJ, Stangl H. SR-BI-mediated high density lipoprotein (HDL) endocytosis leads to HDL resecretion facilitating cholesterol efflux. J Biol Chem. 2006; 281:11193–11204. [PubMed: 16488891]

Pavelka, M.; Ellinger, A. Plattner H Electron microscopy of subcellular dynamics. CDC Press; Boca Raton: 1989. Pre-embedding labeling techniques applicable to intracellular binding sites; p. 199-218.

Pavelka M, Ellinger A, Debbage P, Loewe C, Vetterlein M, Roth J. Endocytic routes to the Golgi apparatus. Histochem Cell Biol. 1998; 109:555–570. [PubMed: 9681635]

Pavelka M, Neumüller J, Ellinger A. Retrograde traffic in the biosynthetic-secretory route. Histochem Cell Biol. 2008; 129:277–288. [PubMed: 18270728]

Rajfur Z, Roy P, Otey C, Romer L, Jacobson K. Dissecting the link between stress fibres and focal adhesions by CALI with EGFP fusion proteins. Nat Cell Biol. 2002; 4:286–293. [PubMed: 11912490]

Sandell JH, Masland RH. Photoconversion of some fluorescent markers to a diaminobenzidine product. J Histochem Cytochem. 1988; 36:555–559. [PubMed: 3356898]

Satoh A, Wang Y, Malsam J, Beard MB, Warren G. Golgin-84 is a rab1 binding partner involved in Golgi structures. Traffic. 2003; 4:153–160. [PubMed: 12656988]

Schmid JA, Scholze P, Kudlacek O, Freissmuth M, Singer EA, Sitte HH. Oligomerization of human serotonin transporter and of the rat GABA transporter 1 visualized by fluorescence resonance energy transfer microscopy in living cells. J Biol Chem. 2001; 276:3805–3810. [PubMed: 11071889]

Singleton CD, Casagrande VA. A reliable and sensitive methode for fluorescent photoconversion. J Neurosci Methods. 1996; 64:47–54. [PubMed: 8869483]

Surrey T, Elowitz MB, Wolf PE, Yang F, Nedelec F, Shokat K, Leibler S. Chromophore-assisted light inactivation and self-organization of microtubules and motors. Proc Natl Acad Sci USA. 1998; 95:4293–4298. [PubMed: 9539730]

Tour O, Meijer RM, Zacharias DA, Adams SR, Tsien RY. Genetically targeted chromophore-assisted light inactivation. Nat Biotech. 2003; 21:1505–1508.

Tsien RY. The green fluorescent protein. Ann Rev Biochem. 1998; 67:509–544. [PubMed: 9759496]

Vetterlein M, Ellinger A, Neumüller J, Pavelka M. Golgi apparatus and TGN during endocytosis. Histochem Cell Biol. 2002; 117:143–150. [PubMed: 11935290]

Vetterlein M, Niapir M, Ellinger A, Neumüller J, Pavelka M. Brefeldin A-regulated retrograde transport into the endoplasmic reticulum of internalised wheat germ agglutinin. Histochem Cell Biol. 2003; 120:121–128. [PubMed: 12883907]

Voelker DR, Kennedy EP. Cellular and enzymic synthesis of sphingomyelin. Biochemistry. 1982; 21:2753–2759. [PubMed: 7093220]

Von Bartheld CS, Cunningham DE, Rubel EW. Neuronal tracing with DiI: decalcification, cryosectioning, and photoconversion of light and electron microscopic analysis. J Histochem Cytochem. 1990; 38:725–733. [PubMed: 2185313]

Yuste R. Fluorescence microscopy today. Nat Methods. 2005; 2:902–904. [PubMed: 16299474]

Europe PMC Funders Author Manuscripts

Europe PMC Funders Author Manuscripts

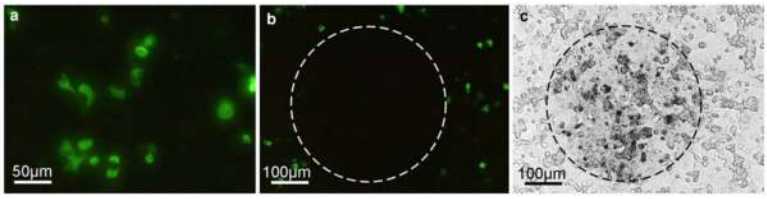

Fig. 1.

Conversion of EGFP-PDI fluorescence signals into DAB-precipitates. The figure shows fluorescence microscopic images of the same field of cultured Hela cells prior to (**a**) and after illumination (**b**), and corresponding to b, the respective phase contrast image (**c**). After illumination, the brightly stained cells visible in **a** are bleached, and hence, no longer visible in the fluorescence microscope (**b**). In parallel, DAB-depositions became apparent (**c**) indicating the successful conversion process

Europe PMC Funders Author Manuscripts

Europe PMC Funders Author Manuscripts

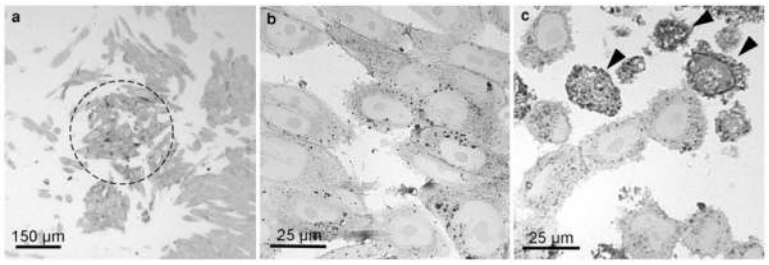

Fig. 2.

Semithin sections of SR-BI-EGFP-expressing ldlA7 cells after photoconversion. The overview shows the darkened cells in the center of the exposed area. The majority of these cells show DAB-deposits, indicating a homogeneous signal conversion. On these sections, the quality of the conversion process is assessed, different staining patterns are listed, and areas of interest for further electron microscopic analyses defined (**a**). The influence of the illumination is shown by the amount of generated DAB-deposits, which increases with the duration of the illumination (**b** 30 minm, **c** 60 min). After 60 min, the percentage of cells with extremely intense reactions is increased (**c** *arrowheads*)

Europe PMC Funders Author Manuscripts

Europe PMC Funders Author Manuscripts

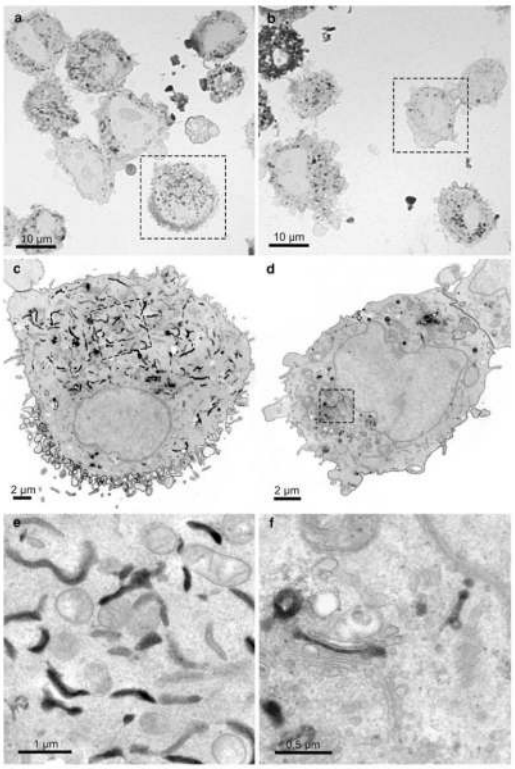

Fig. 3.

Comparison of the SR-BI-EGFP signal in ldlA7 cells after photoconversion on semithin (**a**, **b**) and consecutive thin sections (**c**–**f**) in the light and electron microscope. All cells on the semithin sections show DAB-deposits but the precise localizations cannot be defined at this magnification (**a**, **b**). Electron microscopic analysis of the consecutive ultrathin sections (**a** → **c**→ **e**; **b** → **d** → **f**) clearly show the intracellular reactions mainly confined to the ER (**c**, **e**) and the Golgi apparatus (**d**, **f**), respectively. In all cells, the nuclear envelope remains unstained

Europe PMC Funders Author Manuscripts

Europe PMC Funders Author Manuscripts

Europe PMC Funders Author Manuscripts

Europe PMC Funders Author Manuscripts

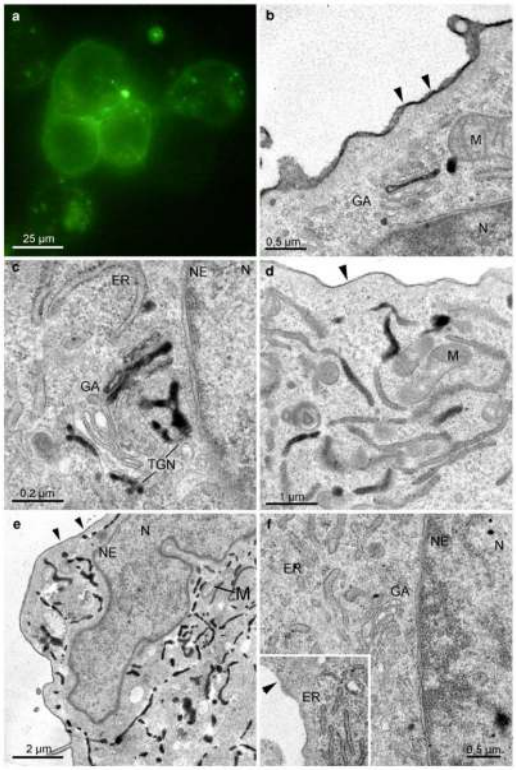

Fig. 4.

Subcellular distribution of the SR-BI-EGFP signal in ldlA7 cells. Fluorescence signals mark the plasma membrane, and distinct cytoplasmic spots (**a**). At the ultrastructural level, the converted signal can be attributed to the PM and to specific cell compartments (**b**–**e**): DAB-deposits are found homogeneously, though with varying intensity, distributed at the PM (**b**, **d**, **e**). Organelle staining is characterized by clear cut reaction products within the Golgi apparatus (**b**, **c**, GA), and the ER (**d**, **e**); the nucleus (*N*), and other organelles, such as mitochondria (*M*), always are negative. At the Golgi stacks different compartments, medial (**b**), *trans*, or the *trans*-Golgi network (*TGN*; **c**) are marked. Two staining patterns prevail in the ER; either are dense deposits found within the entire membrane system of the ER (**e**), or are reactions of different intensities in a mosaic like pattern visible in limited regions of ER-cisternae (**d**). Reaction products never are found within the nuclear envelope (**b**, **c**, **e**; *NE*). Control cells expressing EGFP-SR-BI incubated in DAB without photobleaching lack any reaction products (**f**)

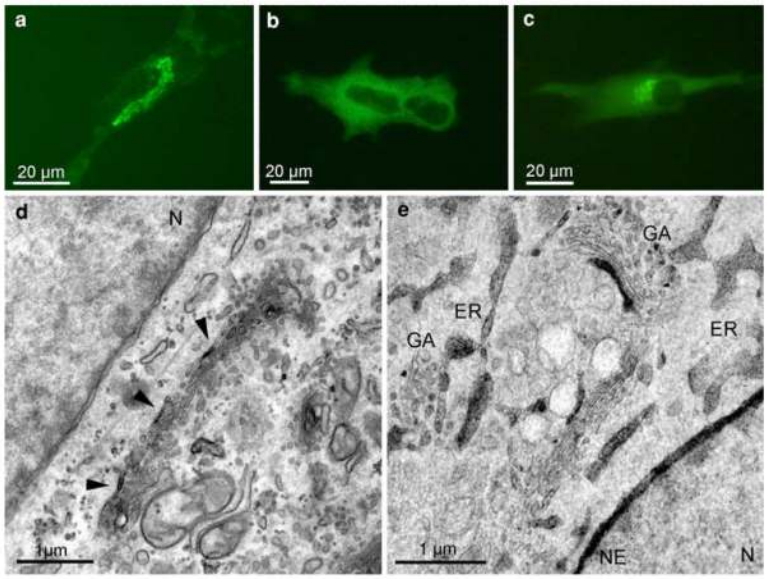

Fig. 5.

EGFP-staining of G-84 and PDI in FSF and HepG2 cells. FSF cells expressing EGFP-G-84 (**a**); HepG2 cells expressing EGFP-PDI (**b**) and co-expressing EGFP-G-84/PDI (**c**). The fluorescence signal of the Golgi marker G-84 is found in the perinuclear Golgi region (**a**), the ER-marker PDI in the entire cytoplasm (**b**), and after co-expression of G-84 and PDI within both, the perinuclear region and distributed throughout the cytoplasm (**c**). After DAB-photoconversion, reaction product of G-84 is restricted to distinct segments of the utmost cisterna at one side of the Golgi stack (**d**, *arrowheads*). Co-expressed G-84 and PDI on the one hand label distinct cisternal segments of the Golgi stacks (**e**, *GA*), on the other hand, endoplasmic reticulum (*ER*) and the nuclear envelope (**e**, *NE*). *N* nucleus

Europe PMC Funders Author Manuscripts
Europe PMC Funders Author Manuscripts

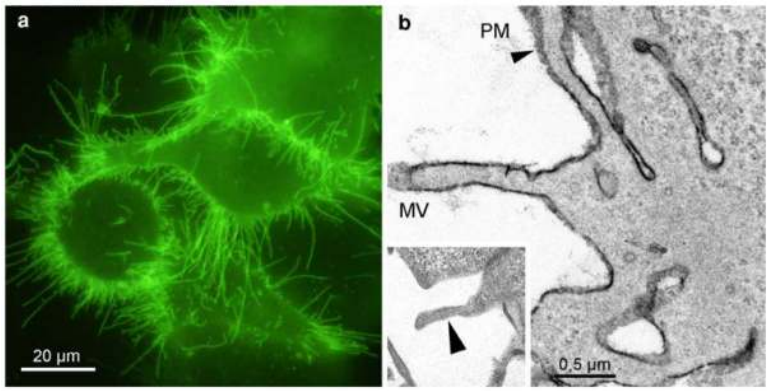

Fig. 6.
YFP-GAT1-staining of Hek293 cells. Strong fluorescence labels the PM, in particular the numerous microvilli (**a**). The staining is confirmed in the electron microscope; after conversion, dense DAB-deposits mark the microvilli (*MV*) and the numerous folds and invaginations of the PM (**b**, *arrowhead*). Control cells, expressing YFP-GAT1, and incubated in DAB without bleaching, are devoid of reaction products (*insert*, *arrowhead*)

Europe PMC Funders Author Manuscripts
Europe PMC Funders Author Manuscripts

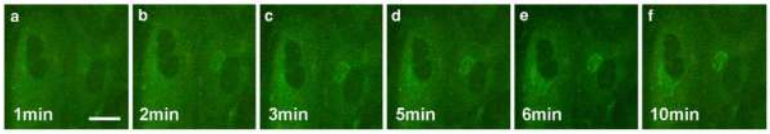

Fig. 7.

Time sequence of BODIPY-cer uptake in FSF cells after surface labelling at 4°C for 30 min. The live cell images show the rapid accumulation of ceramide in the perinuclear Golgi region following warming to 37°C. Scale bar: 25 μm

Europe PMC Funders Author Manuscripts

Europe PMC Funders Author Manuscripts

Europe PMC Funders Author Manuscripts

Europe PMC Funders Author Manuscripts

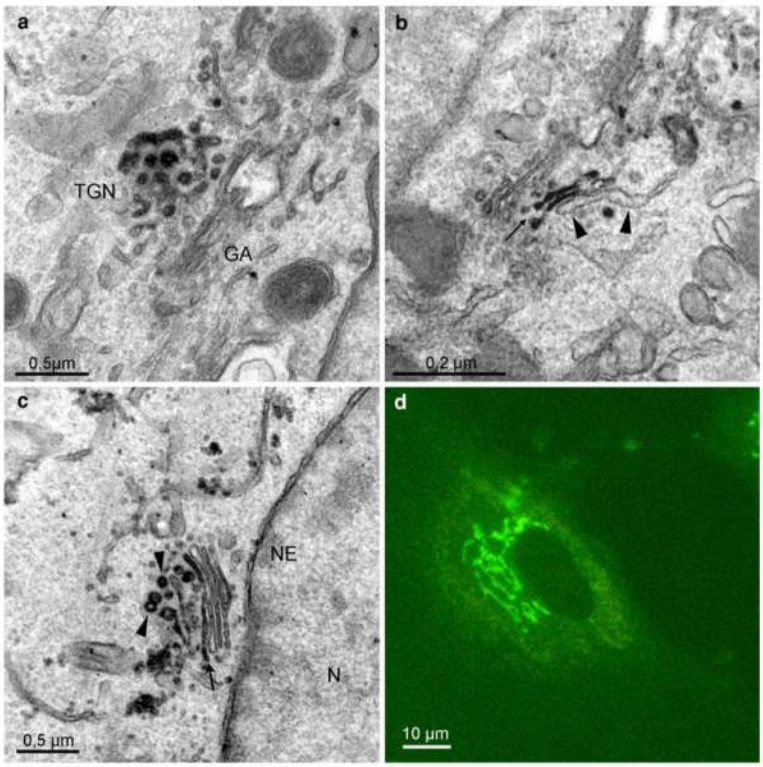

Fig. 8.

Localization of BODIPY-cer in Hela cells, preincubated with BODIPY-cer at 4°C for 5 min. After warming to 37°C for 10 min, reaction product is concentrated in the *trans*-Golgi network (*TGN*, **a**), extending to *trans*-Golgi cisternae (**b**, *arrow*), whereas the *trans*-Golgi ER remains unstained (**b**, *arrowheads*). Further incubation for 30 min at 37°C results in the classical tubulo-reticular perinuclear Golgi staining, seen in the light microscope (**d**). After photoconversion, reaction products mark stacked Golgi cisternae (**c**, *arrow*), as well as cisternal and vesicular membrane profiles of the TGN (**c**, *arrowheads*)

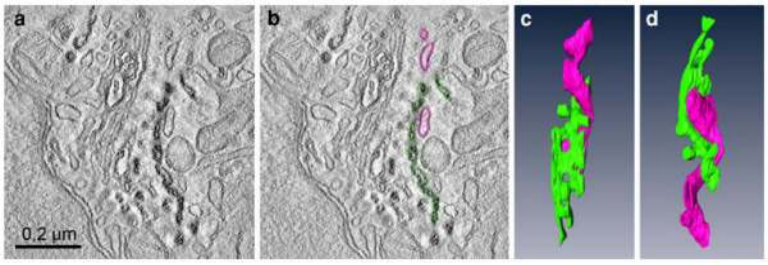

Fig. 9.

Three-dimensional reconstruction of a *trans*-Golgi-ER junction in a HeLa cell labelled with BODIPY-cer at 4°C for 30 min, followed by postincubation at 37° for 10 min. **a** and **b** shows a virtual 2 nm thick slice with (**a**) and without (**b**) coloured contours: **c** and **d** present the respective model in two different aspects. The *trans*-Golgi cisterna, defined by reaction product is coloured green, the negative ER cisterna in *pink*. The different aspects of the 3D-model (**c**, **d**) provide insight into the complex helical organization of the junction. Tubular parts of the *trans*-Golgi ER wind around the multiply perforated *trans*-Golgi cisterna

Europe PMC Funders Author Manuscripts

Europe PMC Funders Author Manuscripts